DISCRET: A SELF-INTERPRETABLE FRAMEWORK FOR TREATMENT EFFECT ESTIMATION

Anonymous authors
Paper under double-blind review

ABSTRACT

Individual treatment effect is of great importance for healthcare and beyond. While most existing solutions focus on accurate treatment effect estimations, they rely on non-interpretable black-box models that can hinder stakeholders from understanding the underlying factors driving the prediction. To address this issue, we propose DISCRET, a self-interpretable framework that is inspired by how stakeholders make critical decisions in practice. DISCRET identifies samples similar to a target sample from a database by using interpretable rules and employs their treatment effect as the estimated ITE for the target sample. We present a deep reinforcement learning-based rule learning algorithm in DISCRET to achieve accurate ITE estimation. We conduct extensive experiments over tabular, natural language, and image settings. Our evaluation shows that DISCRET not only achieves comparable performance as black-box models but also generates more faithful explanations than state-of-the-art post-hoc methods and self-interpretable models.

1 INTRODUCTION

Individual treatment effect (ITE) quantifies the difference between one individual's outcome with and without receiving treatment. Estimating ITE is a significant problem not only in healthcare but also in other domains (Basu et al., 2011; Pryzant et al., 2021; Feder et al., 2021; Jerzak et al., 2023b;a). It serves as an important tool for tailoring interventions to the specific needs of each individual. A substantial body of literature has been dedicated to investigating various methodologies for accurately estimating ITE by harnessing the potential of machine learning and deep learning techniques (Shalit et al., 2017; Yoon et al., 2018; Zhang et al., 2022; Liu et al., 2022).

However, the estimation of ITE confronts a significant challenge with respect to interpretability and explainability. Due to the black-box nature, machine learning models hinder stakeholders from understanding the underlying factors and mechanisms driving treatment effect predictions. Efforts to develop interpretable machine learning methods and frameworks are therefore essential to ensure that ITE estimations are not only accurate but also trustworthy (Kim & Bastani, 2019; Crabbé et al., 2022; Chen et al., 2022).

The state-of-the-art interpretable ITE estimation approaches, while making significant strides in enhancing explainability, often struggle to provide highly accurate ITE estimations (Athey & Imbens, 2016; Nie & Wager, 2021). Additionally, recent studies have made concerted efforts to elucidate the inner workings of black-box models in estimating ITE through post-hoc explanations (Kim & Bastani, 2019). However, post-hoc explanations have also been blamed for their potential lack of faithfulness (Rudin, 2019; Bhalla et al., 2023), which is also empirically validated in Section 4.

To address the above issues, we propose a self-interpretable ITE estimation framework, DISCRET, i.e., "DIScovering Comparable items with Rules to Explain Treatment Effect", for estimating ITE. In line with its nomenclature, DISCRET specializes in estimating ITE for a specific target sample, leveraging the average treatment effect (ATE) estimated from a subgroup of similar samples obtained through rule-based explanations from the database. Typically, this database comprises all training samples. This process is visually elucidated in Figure 1 using an example from the Infant Health and Development Program (IHDP) dataset (Hill, 2011). As depicted in the figure, when determining the impact of high-quality child care (the treatment variable) on an individual subject, such as a premature infant, the initial step involves extracting a group of comparable premature infants from the database using logical rules. Subsequently, the ITE for the target sample is assessed by applying the

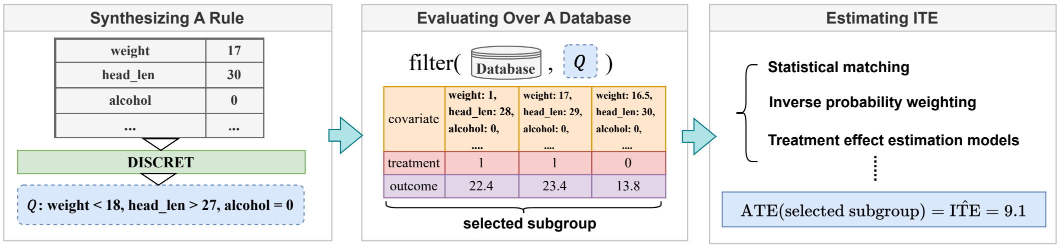
Synthesizing A Rule
weight
17
head_len
30
alcohol
0
...
...
DISCRET
Q: weight < 18, head_len > 27, alcohol = 0
Evaluating Over A Database
filter(Database , Q)
covariate
weight: 1, head_len: 28, alcohol: 0, ...
weight: 17, head_len: 29, alcohol: 0, ...
weight: 16.5, head_len: 30, alcohol: 0, ...
treatment
1
1
0
outcome
22.4
23.4
13.8
selected subgroup
Estimating ITE
Statistical matching
Inverse probability weighting
Treatment effect estimation models
ATE(selected subgroup) = $\hat{\text{ITE}}$ = 9.1

Figure 1: Illustrations of DISCRET using IHDP dataset. To estimate ITE for one sample, DISCRET synthesizes a rule as one explanation, “weight $>$ 1694, head circumference $>$ 27.8, alcohol $=$ 1” which captures a pattern of infants with body weight over 1694 grams, the head circumference over 27.8 centimeters and their mothers taking alcohol during pregnancy. Evaluating this rule over the database retrieves a subgroup of three similar infants. We then estimate the average treatment effect (ATE) over those similar infants as the estimated ITE for the sample shown in the leftmost box.

ATE computed over these similar samples. This approach mirrors the clinical practice of treatment recommendation for individual patients (Seymour et al., 2019), which relies heavily on evaluating treatment effects in patients with analogous characteristics.

To guarantee accurate ITE estimation, we further proposed to leverage Deep reinforcement learning with a novel and tailored reward function for rule learning, which can also overcome the non-differentiability issue caused by the step of evaluating rules over the database. Furthermore, our proposed framework excels in generating inherently more faithful explanations compared to the current state of the art, as quantitatively evaluated through the faithfulness measures introduced by Dasgupta et al. (2022).

We evaluate the capabilities of DISCRET through comprehensive experiments spanning various data domains, including tabular data, text data, and image data, Notably, our approach not only achieves performance levels comparable to black-box models but also excels in producing more faithful explanations than the state of the art. Our contributions can be summarized as follows:

1. We introduce DISCRET, a novel self-interpretable ITE estimation framework that leverages the estimated Average Treatment Effect (ATE) over similar samples retrieved through rule-based explanations for ITE estimation.
2. We present a deep reinforcement learning algorithm tailored for generating explanations specifically designed for ITE estimation.
3. We conduct an extensive series of experiments across diverse data settings, encompassing tabular, text, and image data, providing empirical evidence that DISCRET excels in generating faithful explanations without compromising ITE estimation performance.

2 Background and Problem Statement

We first introduce our problem settings. Suppose each sample consists of (i) the pre-treatment covariate variable X, (ii) the treatment variable T, (iii) a dose variable S associated with T, and (iv) observed outcome Y under treatment T and dose S. Note that we embrace a versatile framework throughout this study, where T can take on either discrete or continuous values, S is inherently continuous but can be either present or absent, Y can be discrete or continuous, and X may incorporate structured features as well as unstructured features, such as text or image data. In the remainder of the paper, we primarily explore the setting where Y is a continuous variable. A generalization of these settings can be found in the Appendix A.

Given the diversity inherent in treatment and dose variables, the range of treatment effects that need estimation also exhibits significant variability. In this paper, we focus on addressing this diversity by delving into three representative settings:

1. Tabular data with a binary treatment variable T and no dose variables. In this setting, $T = 1$ represents treated unit while $T = 0$ represents untreated unit, and the ITE is defined as the difference of outcomes under the treatment and under the control, respectively (i.e., $\text{ITE}(x) = y_1(x) - y_0(x)$, where $y_1(x)$ and $y_0(x)$ represents the potential outcome with and without receiv-

ing treatment for a sample x). The average treatment effect, ATE, is the sample average of ITE across all samples (i.e., ATE $= \mathbb{E}[\text{ITE}]$).

2. Tabular data with a continuous treatment variable T. Following Zhang et al. (2022), the average dose-response function is defined as the treatment effect, i.e., $\mathbb{E}[Y|X, do(T = t)]$.
3. Tabular data with a discrete treatment variable T with one additional continuous dose variable S. Following Zhang et al. (2022), the average treatment effect is defined as the average dose-response function: $\mathbb{E}[Y|X, do(T = t, S = s)]$.

Furthermore, beyond the treatment effect definitions, the propensity score, represented as the probability of treatment assignment T conditioned on the observed covariates X, often plays a pivotal role in regularizing the treatment effect estimation. This propensity score is denoted as $\pi(T|X)$.

Unlike conventional prediction tasks, we are unable to directly observe the counterfactual outcomes during the training phase, rendering the ground-truth treatment effect typically unavailable. To address this challenge and ensure the causal interpretability of our estimated treatment effect, we adhere to the following assumptions proposed by Rubin (1974):

Assumption 1. *(Strong Ignorability/Unconfoundedness) $Y(T = t) \perp T|X$. In the binary treatment case, $Y(0), Y(1) \perp T|X$.*

Assumption 2. *(Positivity/Overlap)* $0 < \pi(T|X) < 1, \forall X, \forall T$.

Assumption 3. *(Consistency) For the binary treatment setting,* $Y = TY(1) + (1 - T)Y(0)$.

For the covariate variable X, we assume that it is composed of m features, $X_1, X_2, \dots, X_m$, which could be the categorical or numeric attributes from tabular data or pre-processed features extracted from the text data or image data. We then build logic rule-based explanations upon those features to construct our treatment effect estimator. Those logic rules are assumed to be in the form of K disjunctions of multiple conjunctions, i.e., R :- $R_1 \vee R_2 \vee \cdots \vee R_H$ where each R_i is a conjunction of K literals: R_i :- $l_{i1} \wedge l_{i2} \wedge l_{i3} \wedge \cdots \wedge l_{iK}$, and :- means if. In the definition of R_i, each $l_{ij}\,(j = 1, 2, \dots)$ represents a literal taking the form of $l_{ij} = (A \ op \ c)$, in which $A \in \{X_1, X_2, ..., X_m\}$, and op is equality for categorical attributes while $op \in \{<, >, =\}$ for numeric attributes.

To facilitate ITE estimation, there are some desired properties for the rule R:

1. **Local interpretability**: We generate rule-based explanations for each individual sample rather than for a population of samples. Thus, the explanations may differ in different patients. Given a target sample with covariate x, we will use R_x to denote the generated rule for this sample. We slightly abuse the notation below by referring to a sample with covariate x as sample x.
2. **Satisfiability**: For any rule R_x used for estimating ITE for the sample x, this sample's covariates should also satisfy this rule. This guarantees that the sample x and similar samples retrieved by rules share the same characteristics.
3. **Low-bias and Non-emptiness**: We expect that R_x can retrieve a set of similar samples so that the bias between the estimated treatment effect over them and the ground-truth ITE is as small as possible, which is referred to as the **Low-bias** property. In addition, there should be at least one sample from the database whose covariates satisfy these rules, which is the **Non-emptiness** property.

Our objective is to estimate the ITE for a given sample x, even in the absence of knowledge regarding its true treatment assignments and outcomes. To achieve this, we aim to develop a rule R_x, which adheres to **Local interpretability**, **Satisfiability**, **Low-bias**, and **Non-emptiness**. Once we have identified and established this rule, we proceed by selecting a subgroup of patients who exhibit similarity according to this rule. Subsequently, we employ the estimated Average Treatment Effect (ATE) computed over this subgroup as the estimated ITE for the sample x.

3 THE FRAMEWORK OF DISCRET

In this section, we provide a step-by-step solution to the rule learning problem as formally introduced in Section 2. Initially, we assume a scenario where each target sample x corresponds to a single disjunction in R_x. Thus, our representation of R_x takes the form of R_x :- $l_1 \wedge l_2 \wedge l_3 \wedge \cdots \wedge l_K$. Within this section, as outlined in Algorithm 1, we commence by elucidating the process of generating R_x and estimating ITE during the inference phase. Subsequently, we delve into the utilization of deep

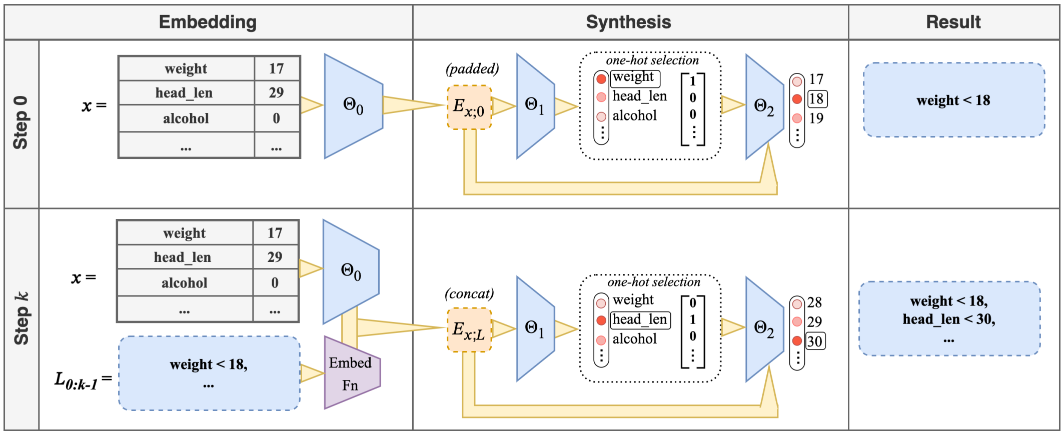

Figure 2: Illustrative overview of the iterative inference forward pass of DISCRET. The model begins at Step 0 by using an embedding of x to generate a single literal For any subsequent step k, the model generates rule L_k by embedding all of the literals generated so far, concatenating it to the embedding for x, generating the next literal, and appending that literal to the rule L_{k-1}.

Algorithm 1 Overview of inference and training phase

```
for each sample with covariate $x$ do
    Generate rule $R_x$ for $x$
    Retrieve similar patients $R_x(\mathcal{D})$ by evaluating $R_x$ on a database $\mathcal{D}$
    if Inference then
        Estimating ATE of $R_x(\mathcal{D})$ as the estimated ITE for $x$
    else if Training then
        Collecting rewards based on $R_x(\mathcal{D})$ and performing Deep Reinforcement Learning
    end if
end for
```

reinforcement learning techniques to effectively learn R_x while ensuring it adheres to the desired properties outlined in Section 2.

3.1 Rule generation at inference phase

DISCRET generates R_x recursively by learning all of $l_k, k = 1, 2, \cdots, K$ one after the other in multiple rounds. Since l_k takes the form of $(A\ op\ c)$, then at each round k, we determine which feature A to select, which constant c to be compared against, and with which operator op.

Figure 2 depicts how a literal l_k is generated at the k_{th} round with one running example from IHDP dataset. First, we encode the covariate x as E_x with one neural network parameterized by Θ_0, and also encode all the literals generated in the first $k-1$ rounds, denoted by "$L_{1:k-1} = \{l_1, l_2, \cdots, l_{k-1}\}$", as E_L. Due to space limit, we leave the details of how to encode $L_{1:k-1}$ to the Appendix A. E_x and E_L are then fed into a feed-forward neural network (parameterized by Θ_1) and *the most probable* feature from $\{X_1, X_2, \ldots, X_m\}$ is selected as A for l_k.

The selection of the constant c and the operator op for literal l_k depends on the type of the selected attribute A. If A is a categorical attribute, then we assign c as $x[A]$, i.e., the value of attribute A in x, and assign op as equality, which can guarantee the **Satisfiability** of R_x on x.

Instead, if A is a numeric attribute, we first discretize the range of A with a list of μ evenly distributed float numbers, $\{C_1, C_2, \ldots, C_\mu\}$. We then design a feed-forward neural network (parameterized by Θ_2) to produce the probability distribution of these μ numbers, which takes the encoding of the covariates, E_x, the encoding of $L_{1:k-1}$, E_L, and the one-hot encoding of feature A as the model input. *The most probable* C_j is then selected as c. We further present the extension of the above rule generation process to multiple disjunctions in Appendix A.

Note that instead of outputting the float number c directly, generating the probability distribution of $|C|$ discrete numbers can facilitate the generation of Q value for deep Q learning. After the feature A and the constant c are identified, the operator *op* is then determined by comparing the value $x[A]$ and c. If $x[A]$ is greater than c, then *op* is assigned as $\geq$ and $\leq$ otherwise. This can again guarantee the **Satisfiability** of the rule R_x on x.

To handle text and image data, one essential step is to extract features from them prior to the above rule generation process, which then become parts of the covariate variables. For text data, we can extract Bag-of-word (BoW) features; for image data, we may follow concept learning methods (Fel et al., 2023; Tran et al., 2022) to extract concept features.

3.2 ITE ESTIMATION AT INFERENCE PHASE

Given a sample x (e.g., a patient) with (x, t, s, y), after generating a rule R_x for a sample x, the next step is to evaluate this rule on a database $\mathcal{D}$ to retrieve a subgroup of similar samples, which is denoted by $R_x(\mathcal{D}) = \{(x_i^*, t_i^*, s_i^*, y_i^*)\}_{i=1}^n$. The ITE of the sample x is then estimated with the average treatment effect (ATE) estimated within this subgroup, which is formulated as below for different types of treatment variables and dose variables:

1. With a binary treatment variable and no dose variable, we can estimate the ATE of $R_x(\mathcal{D})$ via arbitrary treatment effect estimation methods in the literature, such as the classical statistical matching algorithm (Kline & Luo, 2022), or the state-of-the-art neural network models. In this paper, we take the K-Nearest Neighbor Matching by default for estimating ATE of $R_x(\mathcal{D})$: ITE $= y_1(x) - y_0(x)$. We can also obtain the estimated outcome by averaging the outcome of samples from $R_x(\mathcal{D})$ with the same treatment as the sample x, i.e.:

$$\widehat{y}(t) = \frac{1}{\sum \mathbb{I}(t_i^* = t)} \sum \mathbb{I}(t_i^* = t) \cdot y_i^* \tag{1}$$

2. With a continuous treatment variable T but without dose variables, according to Section 2, the ITE is represented by the outcome conditioned on the observed treatment. One straightforward way to estimate it is to employ the average outcome of samples within $R_x(\mathcal{D})$ that receive similar treatments to x, which is also the estimated outcome for this sample:

$$\hat{y} = \frac{\sum \mathbb{I}[(x_i^*, t_i^*, y_i^*) \in \text{top}_k(R_x(\mathcal{D}))] \cdot y_i^*}{\sum \mathbb{I}[(x_i^*, t_i^*, y_i^*) \in \text{top}_k(R_x(\mathcal{D}))]}, \tag{2}$$

in which $\text{top}_k(R_x(\mathcal{D}))$ is constructed by finding the top-k samples from $R_x(\mathcal{D})$ with the most similar treatments to x. But again, any existing treatment effect estimation methods for continuous treatment variables from the literature are applicable to estimate $\widehat{\text{ITE}}_x$.
3. With a discrete treatment variable T and one associated continuous dose variable S, ITE is estimated in a similar way to equation 2, which is included in Appendix A due to space limit.

Note that one implicit assumption that we made here is that the outcome variable is a continuous variable. The generalization of the above formulas to discrete outcome variables is discussed in the appendix. We can also estimate the propensity score for discrete treatment variables by simply calculating the frequency of every treatment within $R_x(\mathcal{D})$: $\widehat{\pi}(T = t|X = x) = \sum \mathbb{I}(t_i^* = t)/|R_x(\mathcal{D})|$:

3.3 TRAINING PHASE

To preserve **low-bias** property, we need to guide the generation of rules such that the estimated ITE is as accurate as possible. We therefore need to optimize this objective by training the three models (Θ_0, Θ_1 and Θ_2) used in the rule generation process. One difficulty of learning $\Theta = [\Theta_0, \Theta_1, \Theta_2]$ is the non-differentiability issue caused by the step of evaluating R_x over the database. We overcome this issue by formulating this model training problem as a deep reinforcement learning (RL) problem, and propose to adapt deep Q learning (DQL) algorithm to solve this problem.

RL problem formulation We first map the notations from Section 3.1 to classical RL terminology. An RL agent takes one *action* at one *state*, collects a *reward* from the environment, which is then transitioned to a new state. In our rule learning setting, a *state* is composed of the covariates x and the generated literals in the first $k-1$ rounds, $L_{1:k-1}$. With x and $L_{1:k-1}$, the model Θ_1 and Θ_2 collectively determine the k_{th} literal, l_k, which is regarded as one *action*. Our goal is then to learn a policy parameterized by Θ, which models the probability distribution of all possible l_k conditioned on the state $(x, L_{1:k-1})$, such that the value function calculated over all K rounds is maximized:

$$V_{1:K} = \sum\nolimits_{k=1}^{K} r_k \gamma^{k-1}, \tag{3}$$

in which γ is a discounting factor. Note that there are only K horizons/rounds in our settings since the number of conjunctions in the generated rules is limited. To bias rule generation towards accurate estimation of ITE, we expect that the value function $V_{1:K}$ reflects how small the ITE estimation error is. However, since the counterfactual outcomes are not observed in the training phase, we therefore use the errors of the observed outcomes as a surrogate of the ITE estimation error. Also, we give a zero reward to the case where the retrieved subgroup, $L_{1:K}(\mathcal{D})$, is empty after evaluating $L_{1:K}$ on the database $\mathcal{D}$, which can thus guarantee the **non-emptiness** of the rules. As a result, $V_{1:K}$ is formulated as

$$V_{1:K} = e^{-\alpha(y-\widehat{y}_{1:K})^2} \cdot \mathbb{I}(|L_{1:K}(\mathcal{D})| > 0), \tag{4}$$

in which $\widehat{y}_{1:K}$ represents the estimated outcome by using the generated rule composed of literals $L_{1:K}$ and α is a hyper-parameter. As a consequence, the reward collected at the k_{th} round of generating l_k becomes $r_k = (V_{1:k} - V_{1:k-1})/\gamma^{k-1}$.

Deep Q learning for model training To maximize the value function $V_{1:K}$, Deep Q learning (DQL) (Mnih et al., 2013) is employed to learn the parameter Θ. To facilitate Q learning, we estimate the Q value with the output logits of the models given a state $(x, L_{1:k-1})$ and an action l_k. Further details on how to employ Deep Q learning for model training are included in Appendix A.

We further present some strategies to optimize the design of the cumulative reward function defined in equation 4, which includes incorporating estimated propensity scores into this formula and automatically fine-tuning its hyper-parameters.

Regularization by estimating propensity scores First of all, similar to prior studies on ITE estimation (Shi et al., 2019; Zhang et al., 2022), we regularize the reward function r_k by integrating the estimated propensity score, $\widehat{\pi}(T = t|X = x)$. Specifically, for discrete treatment variables, we reweight equation 5 with the propensity score as a regularized reward function, i.e.:

$$V_{1:K}^{reg} = [e^{-\alpha(y-\widehat{y}_{1:K})^2} + \beta \cdot \widehat{\pi_{1:k}}(T = t|X = x)] \cdot \mathbb{I}(|L_{1:K}(\mathcal{D})| > 0), \tag{5}$$

Automatic hyper-parameter fine-tuning We further studied how to automatically tune the hyper-parameter α and β in equation 5. For α, at each training epoch, we identify the training sample producing the median of $(y - \widehat{y}_{1:K})^2$ among the whole training set and then ensure that for this sample, equation 4 is 0.5 through adjusting α. This can guarantee that for those training samples with the smallest or largest outcome errors, equation 4 approaches 1 or 0 respectively.

We further design an annealing strategy to dynamically adjust β by setting it as 1 during the initial training phase to focus more on treatment predictions, and switching it to 0 so that reducing outcome error is prioritized in the subsequent training phase.

4 Experiments

4.1 Experimental settings

Datasets The experiments are conducted across tabular, NLP, and image settings.

In the context of tabular data settings, we conduct comprehensive evaluations across the settings with diverse categories of treatment variables. Specifically, we have selected the following datasets for our evaluation: the IHDP dataset (Hill, 2011), featuring a binary treatment variable without dose variables; the TCGA dataset (Weinstein et al., 2013), which includes multiple discrete treatment options and continuous dosage information; and two additional datasets, IHDP-C (a variant of IHDP) and News, both containing continuous treatment variables but lacking dose-related information.

For text data, we conducted experiments on the Enriched Equity Evaluation Corpus dataset, abbreviated as EEEC designed to explore the impact of treatment variables, specifically changes in racial and gender-related nouns, on the predictions of five distinct mood states for individual sentences. Within our experiments, we consider two variants of this dataset, each focusing on racial nouns and gender-related nouns respectively, denoted as EEEC (Race) and EEEC (Gender) respectively.

In our exploration of image data, we utilized a satellite image dataset enriched with associated covariates, originating from various regions of Uganda, succinctly referred to as Uganda (Jerzak et al., 2023b;a). This dataset was used to investigate the potential impact of grant assignments, considered as the treatment variable, on the aggregated summary of skilled labor in the respective regions. The detailed description of these datasets is included in Appendix C.

Baseline methods We consider the following categories of baseline methods. For neural network models, we used TransTEE (Zhang et al., 2022), Dragonnet (Shi et al., 2019), TARNet (Shalit et al., 2017), Ganite (Yoon et al., 2018), DRNet (Schwab et al., 2020), and VCNet (Nie et al., 2020). Note that Ganite and VCNet can only handle binary treatments without dose variables, which are thus not applied to TCGA, IHDP-C, and News dataset.

We also consider self-interpretable models such as logistic regression (LR), decision tree (DT), and random forests (RF) model, which are integrated into R-learner (Nie & Wager, 2021) for causal inference. For tree-based models, we limit the complexity (e.g., the number of trees and tree depths) to be the same as DISCRET for fair comparison. In addition, we adapted three self-interpretable models designed for general prediction tasks to ITE estimations. These three models include ENRL (Shi et al., 2022), ProtoVAE (Gautam et al., 2022)[1] and Neural Additive Model (NAM) (Agarwal et al., 2021), which generate rules, prototypes and feature attributes as explanations respectively.

We further compare DISCRET against post-hoc explainers, including Lore (Guidotti et al., 2018), Anchor (Ribeiro et al., 2018), Lime (Ribeiro et al., 2016), Shapley values (Shrikumar et al., 2017) and decision tree-based model distillation methods (Frosst & Hinton, 2017) (Model Distillation for short). In the experiments, we apply these methods to the TransTEE model during test time.

Evaluation metrics The first type of metrics is for evaluating ITE estimation performance. For the datasets with binary treatment variables, by following prior studies (Shi et al., 2019; Shalit et al., 2017), the absolute error in average treatment effect, i.e.,: $\epsilon_{ATE} = |\frac{1}{n}\sum_{i=1}^{n} ITE(x_i) - \frac{1}{n}\sum_{i=1}^{n}\widehat{ITE}(x_i)|$, is employed for evaluations. Both in-sample and out-of-sample ϵ_{ATE} are reported. For the datasets with either continuous dose variables or continuous treatment variables, we follow (Zhang et al., 2022) to report the average mean square errors $AMSE$ between the ground-truth outcome and predicted outcome on the test set. The definition of $AMSE$ is provided in Appendix F. For the image dataset, Uganda, since there is no ground-truth ITE, we therefore only report the average outcome errors between the ground-truth outcomes and the predicted outcomes conditioned on observed treatments, i.e., $\epsilon_{\text{outcome}} = \frac{1}{n}\sum_{i=1}^{n}|y_i - \hat{y}_i|$.

We further compare the *faithfulness* of the explanations produced by DISCRET, the post-hoc explainers, and self-interpretable models. Specifically, we leverage two faithfulness metrics, *consistency* and *sufficiency*, proposed by (Dasgupta et al., 2022). Roughly speaking, *Consistency* quantifies how consistent the model predictions are between samples with the same explanations while *sufficiency* generalizes this notion of consistency to arbitrary samples satisfying the same explanations (but not necessarily producing the same explanations). The formal definition of these two metrics and how to evaluate them are discussed in Appendix F.

Configurations for DISCRET We perform grid search on the number of conjunctions,K, and the number of disjunctions, H. We incorporate the propensity score regularization and auto-tuning on α and β. But we also performed an ablation study in Appendix D to study how these optimizations on the reward functions influence the ITE estimation performance.

Extracting features from text and image data For text data, we employ the word frequency features such as "Term Frequency-Inverse Document Frequency" (Baeza-Yates et al., 1999). For image data, we follow (Fel et al., 2023) to extract interpretable concepts as the features, which is discussed in Appendix E in detail.

[1] note that ProtoVAE is designed for image data. We therefore only compare DISCRET against this method in Uganda dataset

Modality →	**Tabular**					**Text**	**Image**
Dataset →	IHDP		TCGA		IHDP-C	EEEC (Race)	Uganda
Method ↓	ϵ_{ATE} (In-sample)	ϵ_{ATE} (Out-of-sample)	ϵ_{ATE} (In-sample)	ϵ_{ATE} (Out-of-sample)	AMSE	ϵ_{ATE}	$\epsilon_{\text{outcome}}$
LR	3.366±2.189	2.497±1.814	31.737±0.001	57.541±0.001	36.640±16.455	0.014±0.016	1.796±0.021
DT	0.345±0.273	0.530±0.399	0.200±0.012	0.202±0.012	22.136±1.741	0.014±0.016	1,796±0.021
RF	0.739±0.284	0.737±0.383	0.263±0.057	0.264±0.058	21.348±1.222	0.525±0.573	1.820±0.013
NAM	0.225±0.221	0.519±0.512	4.201±0.232	4.211±0.152	24.706±0.756	0.152±0.041	1.710±0.098
ENRL	4.160±1.060	4.439±1.587	10.938±2.019	10.942±2.019	24.720±0.985	-	1.800±0.143
Dragonnet	0.177±0.139	0.219±0.143	-	-	-	0.011±0.018	1.709±0.127
TARNet	0.186±0.130	0.408±0.418	1.421±0.078	1.421±0.078	12.967±1.781	0.009±0.018	1.743±0.135
Ganite	1.127±0.481	1.144±0.352	-	-	-	1.998±0.016	1.766±0.024
DRNet	0.188±0.132	0.407±0.422	1.374±0.086	1.374±0.085	11.071±0.994	0.008±0.018	1.748±0.127
VCNet	4.205±0.569	4.434±0.851	0.292±0.074	0.292±0.074	-	0.011±0.017	1.890±0.110
TransTEE	**0.128±0.103**	**0.203±0.130**	**0.055±0.014**	**0.056±0.013**	**0.488±0.288**	0.003±0.017	1.707±0.158
DISCRET	0.274±0.253	0.344±0.303	0.076±0.019	0.077±0.020	0.801±0.165	**0.000±0.017**	**1.662±0.136**

Table 1: ITE estimation errors (lower is better). We **bold** the smallest estimation error for each dataset and underline the smallest among the self-interpretable methods. DISCRET outperforms existing self-interpretable methods on 6 out of the 7 benchmarks.

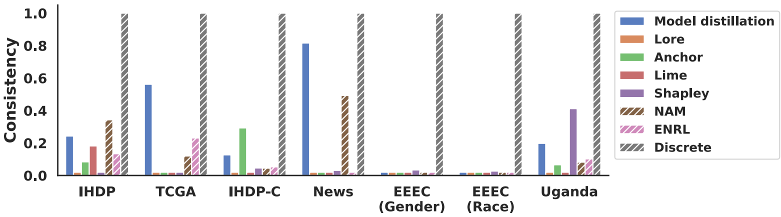

Figure 3: The comparison of the consistency scores between different explanation methods across different datasets. Larger is better.

4.2 Quantitative ITE estimation performance

We include the ITE estimation results for tabular setting, NLP setting, and image setting in Table 1. In this table, we bold and underline those performance numbers that are the smallest prediction errors (or closest to the ground-truth ATE) among all the methods and all the self-interpretable methods respectively. Due to the space limit, the results on News dataset and EEEC (Gender) dataset are not reported in Table 1, which are included in Table 3 and 5 respectively in Appendix G.

As Table 1 shows, DISCRET outperforms all the self-interpretable methods most times, thus demonstrating the performance advantage of DISCRET over these methods. By comparing against black-box models, DISCRET only performs slightly worse than black-box models in most cases. DISCRET can even outperform them on Uganda dataset, which is possibly caused by the overfitting issue encountered by those black-box models due to the small size of Uganda.

4.3 Quantitative explanation quality evaluations

We evaluate the *consistency* and *sufficiency* on the explanations produced by DISCRET, the state-of-the-art self-interpretable models, and the post-hoc explainers. For those explainers producing feature-based explanations, we also follow (Dasgupta et al., 2022) to discretize the feature importance scores, say, by selecting the Top-K most important features, for identifying samples with exactly the same explanations. For fair comparison, we evaluate the explanations generated w.r.t. the same set of features extracted from NLP and image data.

Due to the space limit, we only report the consistency scores of different explanation methods across all the settings, in Figure 3. The full consistency scores are included in Table 4 in Appendix G. As this figure indicates, DISCRET always achieves 100% consistency since the same explanations in DISCRET always retrieve the same subgroup from the database, thus generating the same model predictions. In contrast, the baseline explanation methods generally have extremely low consistency scores in most cases. We also include the sufficiency score results in Table 7, which shows that DISCRET can still obtain higher sufficiency scores in most cases than other explanation methods.

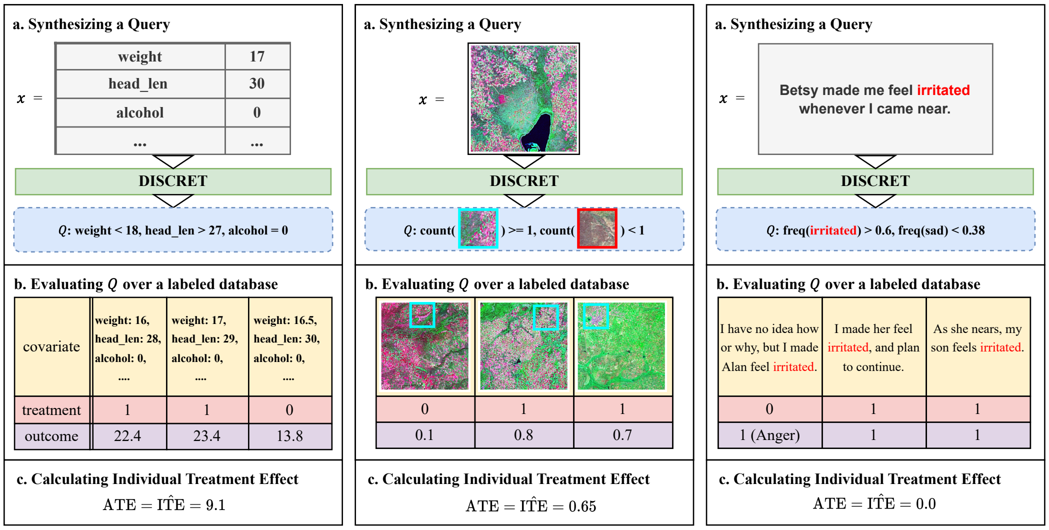
a. Synthesizing a Query
x =
DISCRET
b. Evaluating Q over a labeled database
c. Calculating Individual Treatment Effect

weight	17
head_len	30
alcohol	0
...	...

Q: weight < 18, head_len > 27, alcohol = 0

covariate	weight: 16, head_len: 28, alcohol: 0, ...	weight: 17, head_len: 29, alcohol: 0, ...	weight: 16.5, head_len: 30, alcohol: 0, ...
treatment	1	1	0
outcome	22.4	23.4	13.8

$\mathrm{ATE} = \hat{\mathrm{ITE}} = 9.1$

Q: count( ) >= 1, count( ) < 1

0	1	1
0.1	0.8	0.7

$\mathrm{ATE} = \hat{\mathrm{ITE}} = 0.65$

Betsy made me feel irritated whenever I came near.

Q: freq(irritated) > 0.6, freq(sad) < 0.38

I have no idea how or why, but I made Alan feel irritated.	I made her feel irritated, and plan to continue.	As she nears, my son feels irritated.
0	1	1
1 (Anger)	1	1

$\mathrm{ATE} = \hat{\mathrm{ITE}} = 0.0$

Figure 4: Qualitative examples from IHDP, EEEC and Uganda dataset.

4.4 Qualitative analysis

We perform qualitative studies on some representative examples from tabular setting (IHDP dataset), NLP setting (EEEC dataset), and image setting (Uganda dataset) (shown in Figure 4) to explore whether the learned rules are reasonable or not. For the example from EEEC dataset, "Betsy made me feel irritated whenever I came near" shown in Figure 4, DISCRET generated the following rule constructed over the word frequency features, "freq(irritated) $>$ 0.06, freq(sad) $<$ 0.38". This indicates that sentences following this rule should have non-zero occurrence of the word "irritated" and not too many occurrences of "sad". The evaluation of this rule thus returns three sentences from the database, which all contain the word "irritated". Since the word "irritate" is highly correlated with the mood "Anger", the change of the "Gender" or "Race" nouns won't actually affect the mood of the whole sentence, which matches the ground-truth labels. As a result, the estimated ATE over the subgroup and thus the estimated ITE for this example sentence is 0. For the example from Uganda dataset shown in Figure 4, we leave the analysis to Appendix H due to space limit.

5 Related work

Treatment effect estimation A substantial body of research has been dedicated to the estimation of treatment effects through machine learning. For instance, Shalit et al. (2017) introduced a novel theoretical analysis and a comprehensive family of algorithms to predict ITE from observational data. Additionally, Wager & Athey (2018) pioneered the introduction of a non-parametric causal forest approach tailored for the estimation of heterogeneous treatment effects. Moreover, bridging the gap between the predictive power of machine learning models and the need for interpretable decisions remains a pivotal challenge. To address the issue, Kim & Bastani (2019) proposed a framework for learning interpretable models from observational data for predicting ITE.

Due to space limit, we further discuss related work on **Model interpretability** in Appendix B.

6 Conclusion

In this work, we introduce a self-interpretable framework, DISCRET, for ITE estimation. Within the DISCRET framework, we not only focus on accurate ITE estimation but also prioritize the generation of faithful explanations. To achieve this, we have developed a specialized deep reinforcement learning algorithm that is tailored to the task of generating these explanations. Extensive experiments across different data modalities demonstrate that DISCRET can balance the ITE estimation performance and the faithfulness in explanations.

REFERENCES

Radhakrishna Achanta, Appu Shaji, Kevin Smith, Aurelien Lucchi, Pascal Fua, and Sabine Süsstrunk. Slic superpixels compared to state-of-the-art superpixel methods. *IEEE transactions on pattern analysis and machine intelligence*, 34(11):2274–2282, 2012.

Rishabh Agarwal, Levi Melnick, Nicholas Frosst, Xuezhou Zhang, Ben Lengerich, Rich Caruana, and Geoffrey E Hinton. Neural additive models: Interpretable machine learning with neural nets. *Advances in neural information processing systems*, 34:4699–4711, 2021.

Susan Athey and Guido Imbens. Recursive partitioning for heterogeneous causal effects. *Proceedings of the National Academy of Sciences*, 113(27):7353–7360, 2016.

Ricardo Baeza-Yates, Berthier Ribeiro-Neto, et al. *Modern information retrieval*, volume 463. ACM press New York, 1999.

Anirban Basu, Daniel Polsky, and Willard G Manning. Estimating treatment effects on healthcare costs under exogeneity: is there a 'magic bullet'? *Health Services and Outcomes Research Methodology*, 11:1–26, 2011.

Usha Bhalla, Suraj Srinivas, and Himabindu Lakkaraju. Verifiable feature attributions: A bridge between post hoc explainability and inherent interpretability. In *ICML 3rd Workshop on Interpretable Machine Learning in Healthcare (IMLH)*, 2023.

Ioana Bica, James Jordon, and Mihaela van der Schaar. Estimating the effects of continuous-valued interventions using generative adversarial networks. *Advances in Neural Information Processing Systems*, 33:16434–16445, 2020.

Kan Chen, Qishuo Yin, and Qi Long. Covariate-balancing-aware interpretable deep learning models for treatment effect estimation. *arXiv preprint arXiv:2203.03185*, 2022.

Jonathan Crabbé, Alicia Curth, Ioana Bica, and Mihaela van der Schaar. Benchmarking heterogeneous treatment effect models through the lens of interpretability. *Advances in Neural Information Processing Systems*, 35:12295–12309, 2022.

Sanjoy Dasgupta, Nave Frost, and Michal Moshkovitz. Framework for evaluating faithfulness of local explanations. In *International Conference on Machine Learning*, pp. 4794–4815. PMLR, 2022.

Avinash K Dixit. *Optimization in economic theory*. Oxford University Press, USA, 1990.

Amir Feder, Nadav Oved, Uri Shalit, and Roi Reichart. Causalm: Causal model explanation through counterfactual language models. *Computational Linguistics*, 47(2):333–386, 2021.

Thomas Fel, Victor Boutin, Mazda Moayeri, Rémi Cadène, Louis Bethune, Mathieu Chalvidal, Thomas Serre, et al. A holistic approach to unifying automatic concept extraction and concept importance estimation. *arXiv preprint arXiv:2306.07304*, 2023.

Nicholas Frosst and Geoffrey Hinton. Distilling a neural network into a soft decision tree. *arXiv preprint arXiv:1711.09784*, 2017.

Srishti Gautam, Ahcene Boubekki, Stine Hansen, Suaiba Salahuddin, Robert Jenssen, Marina Höhne, and Michael Kampffmeyer. Protovae: A trustworthy self-explainable prototypical variational model. *Advances in Neural Information Processing Systems*, 35:17940–17952, 2022.

Riccardo Guidotti, Anna Monreale, Salvatore Ruggieri, Dino Pedreschi, Franco Turini, and Fosca Giannotti. Local rule-based explanations of black box decision systems. *arXiv preprint arXiv:1805.10820*, 2018.

Jennifer L Hill. Bayesian nonparametric modeling for causal inference. *Journal of Computational and Graphical Statistics*, 20(1):217–240, 2011.

Connor T Jerzak, Fredrik Johansson, and Adel Daoud. Image-based treatment effect heterogeneity. *arXiv preprint arXiv:2206.06417*, 2022.

Connor T. Jerzak, Fredrik Johansson, and Adel Daoud. Integrating earth observation data into causal inference: Challenges and opportunities. *ArXiv Preprint*, 2023a.

Connor T. Jerzak, Fredrik Johansson, and Adel Daoud. Image-based treatment effect heterogeneity. *Proceedings of the Second Conference on Causal Learning and Reasoning (CLeaR), Proceedings of Machine Learning Research (PMLR)*, 213:531–552, 2023b.

Carolyn Kim and Osbert Bastani. Learning interpretable models with causal guarantees. *arXiv preprint arXiv:1901.08576*, 2019.

Adrienne Kline and Yuan Luo. Psmpy: a package for retrospective cohort matching in python. In *2022 44th Annual International Conference of the IEEE Engineering in Medicine & Biology Society (EMBC)*, pp. 1354–1357. IEEE, 2022.

Qiao Liu, Zhongren Chen, and Wing Hung Wong. Causalegm: a general causal inference framework by encoding generative modeling. *arXiv preprint arXiv:2212.05925*, 2022.

Volodymyr Mnih, Koray Kavukcuoglu, David Silver, Alex Graves, Ioannis Antonoglou, Daan Wierstra, and Martin Riedmiller. Playing atari with deep reinforcement learning. *arXiv preprint arXiv:1312.5602*, 2013.

David Newman. Bag of Words. UCI Machine Learning Repository, 2008. DOI: https://doi.org/10.24432/C5ZG6P.

Lizhen Nie, Mao Ye, Dan Nicolae, et al. Vcnet and functional targeted regularization for learning causal effects of continuous treatments. In *International Conference on Learning Representations*, 2020.

Xinkun Nie and Stefan Wager. Quasi-oracle estimation of heterogeneous treatment effects. *Biometrika*, 108(2):299–319, 2021.

Reid Pryzant, Dallas Card, Dan Jurafsky, Victor Veitch, and Dhanya Sridhar. Causal effects of linguistic properties. In *Proceedings of the 2021 Conference of the North American Chapter of the Association for Computational Linguistics: Human Language Technologies*, pp. 4095–4109, 2021.

Alec Radford, Jong Wook Kim, Chris Hallacy, Aditya Ramesh, Gabriel Goh, Sandhini Agarwal, Girish Sastry, Amanda Askell, Pamela Mishkin, Jack Clark, et al. Learning transferable visual models from natural language supervision. In *International conference on machine learning*, pp. 8748–8763. PMLR, 2021.

Marco Tulio Ribeiro, Sameer Singh, and Carlos Guestrin. " why should i trust you?" explaining the predictions of any classifier. In *Proceedings of the 22nd ACM SIGKDD international conference on knowledge discovery and data mining*, pp. 1135–1144, 2016.

Marco Tulio Ribeiro, Sameer Singh, and Carlos Guestrin. Anchors: High-precision model-agnostic explanations. In *Proceedings of the AAAI conference on artificial intelligence*, volume 32, 2018.

Donald B Rubin. Estimating causal effects of treatments in randomized and nonrandomized studies. *Journal of educational Psychology*, 66(5):688, 1974.

Cynthia Rudin. Stop explaining black box machine learning models for high stakes decisions and use interpretable models instead. *Nature machine intelligence*, 1(5):206–215, 2019.

Patrick Schwab, Lorenz Linhardt, Stefan Bauer, Joachim M Buhmann, and Walter Karlen. Learning counterfactual representations for estimating individual dose-response curves. In *Proceedings of the AAAI Conference on Artificial Intelligence*, volume 34, pp. 5612–5619, 2020.

Christopher W Seymour, Jason N Kennedy, Shu Wang, Chung-Chou H Chang, Corrine F Elliott, Zhongying Xu, Scott Berry, Gilles Clermont, Gregory Cooper, Hernando Gomez, et al. Derivation, validation, and potential treatment implications of novel clinical phenotypes for sepsis. *Jama*, 321(20):2003–2017, 2019.

Uri Shalit, Fredrik D Johansson, and David Sontag. Estimating individual treatment effect: generalization bounds and algorithms. In *International conference on machine learning*, pp. 3076–3085. PMLR, 2017.

Claudia Shi, David Blei, and Victor Veitch. Adapting neural networks for the estimation of treatment effects. *Advances in neural information processing systems*, 32, 2019.

Shaoyun Shi, Yuexiang Xie, Zhen Wang, Bolin Ding, Yaliang Li, and Min Zhang. Explainable neural rule learning. In *Proceedings of the ACM Web Conference 2022*, pp. 3031–3041, 2022.

Avanti Shrikumar, Peyton Greenside, and Anshul Kundaje. Learning important features through propagating activation differences. In *International conference on machine learning*, pp. 3145–3153. PMLR, 2017.

Thien Q Tran, Kazuto Fukuchi, Youhei Akimoto, and Jun Sakuma. Unsupervised causal binary concepts discovery with vae for black-box model explanation. In *Proceedings of the AAAI Conference on Artificial Intelligence*, volume 36, pp. 9614–9622, 2022.

Stefan Wager and Susan Athey. Estimation and inference of heterogeneous treatment effects using random forests. *Journal of the American Statistical Association*, 113(523):1228–1242, 2018.

Jianhao Wang, Zhizhou Ren, Beining Han, Jianing Ye, and Chongjie Zhang. Towards understanding cooperative multi-agent q-learning with value factorization. *Advances in Neural Information Processing Systems*, 34:29142–29155, 2021.

John N Weinstein, Eric A Collisson, Gordon B Mills, Kenna R Shaw, Brad A Ozenberger, Kyle Ellrott, Ilya Shmulevich, Chris Sander, and Joshua M Stuart. The cancer genome atlas pan-cancer analysis project. *Nature genetics*, 45(10):1113–1120, 2013.

Jinsung Yoon, James Jordon, and Mihaela Van Der Schaar. Ganite: Estimation of individualized treatment effects using generative adversarial nets. In *International conference on learning representations*, 2018.

Yi-Fan Zhang, Hanlin Zhang, Zachary C Lipton, Li Erran Li, and Eric P Xing. Exploring transformer backbones for heterogeneous treatment effect estimation. *arXiv preprint arXiv:2202.01336*, 2022.